

# Better Teacher Better Student: Dynamic Prior Knowledge for Knowledge Distillation

Zengyu Qiu<sup>\*1</sup>, Xinzhu Ma<sup>\*1,2</sup>, Kunlin Yang<sup>\*†1</sup>, Chunya Liu<sup>1</sup>,  
Jun Hou<sup>1</sup>, Shuai Yi<sup>1</sup>, Wanli Ouyang<sup>2</sup>

<sup>1</sup>SenseTime Research, <sup>2</sup>The University of Sydney, SenseTime Computer Vision Group  
{liuchunya, yangkunlin}@sensetime.com, {xinzhu.ma, wanli.ouyang}@sydney.edu.au

## Abstract

Knowledge distillation (KD) has shown very promising capabilities in transferring learning representations from large models (teachers) to small models (students). However, as the capacity gap between students and teachers becomes larger, existing KD methods fail to achieve better results. Our work shows that the ‘prior knowledge’ is vital to KD, especially when applying large teachers. Particularly, we propose the dynamic prior knowledge (DPK), which integrates part of teacher’s features as the prior knowledge before the feature distillation. This means that our method also takes the teacher’s feature as ‘input’, not just ‘target’. Besides, we dynamically adjust the ratio of the prior knowledge during the training phase according to the feature gap, thus guiding the student in an appropriate difficulty. To evaluate the proposed method, we conduct extensive experiments on two image classification benchmarks (*i.e.* CIFAR100 and ImageNet) and an object detection benchmark (*i.e.* MS COCO). The results demonstrate the superiority of our method in performance under varying settings. More importantly, our DPK makes the performance of the student model positively correlated with that of the teacher model, which means that we can further boost the accuracy of students by applying larger teachers. Our codes will be publicly available for the reproducibility.

## 1 Introduction

Tremendous efforts have been made in crafting lightweight deep neural networks applicable to the real-world scenarios. Representative methods include network pruning [18], model quantization [16], neural architecture search (NAS) [55], and knowledge distillation (KD) [4, 22], *etc.* Among them, KD has recently emerged as one of the most flourishing topics due to its effectiveness [34, 65, 7, 20] and wide applications [59, 10, 35, 61].

Particularly, the core idea of KD is to transfer the distilled knowledge from a well-performed but cumbersome teacher to a compact and lightweight students. Based on this, lots of methods are proposed and achieve great success. However, with the deepening of research, some related issues are also discussed. In particular, several papers [9, 39, 22, 34] report that with the increase of teacher model in performance, the accuracy of student gets saturated (which might be unsurprising). To make matters worse, in playing the role of teacher, the large teacher models lead to significantly worse performance than the relatively smaller ones. For example, as shown in Fig. 1, ICKD [34], a strong baseline model which also reports this issue, performs better under the guidance of ResNet-101, while applying ResNet-152 as the teacher will degrade the student significantly.

Same as [9, 39], we attribute the cause of this issue to the capacity gap between the teachers and the students. More specifically, the small student is hard to ‘understand’ the high-order semantics

<sup>\*</sup>Equal contribution. <sup>†</sup>Corresponding author.

extracted by the large model, and this problem will be exacerbated when applying larger teachers, which makes the student’s accuracy inversely correlated with the capacity of the teacher model. Note that this problem also exists for humans, and human teachers often tell students some *prior knowledge* in this case. Moreover, the experienced teachers can also *adjust* the amounts of provided prior knowledge accordingly for different students to fully develop their potentials.

Inspired by the human teacher paradigm described above, we propose the dynamic prior knowledge (DPK) framework for feature distillation. Specifically, to provide the student with prior knowledge, we replace its features at some random spatial positions with corresponding teacher features at the same positions. Besides, we further design a ViT [14]-based module to fully integrate these ‘prior knowledge’ with the student’s features. Furthermore, our method also dynamically adjust the amounts of the prior knowledge, reflecting in the ratios of teacher’s features in the hybrid feature map. Particularly, DPK captures the differences of features between the student and the teacher in the training phase, and dynamically updates the feature ratio. In this way, the student always learns from the teacher under an appropriate difficulty, avoiding the performance degradation mentioned in the previous paragraphs.

We evaluate DPK on two image classification benchmarks (*i.e.*, CIFAR-100 [28] and ImageNet[12]) and an object detection benchmark (*i.e.*, MS COCO [31]). Experimental results indicate that DPK outperforms other baseline models under fair settings. More importantly, our method can be further improved by applying better teachers (see Fig. 1 for an example). We argue that this feature of our model not only further boosts performance, but also provides a solution to the “trade-off” between model size and accuracy in teacher selection. In addition, we perform extensive ablation to elaborate each design of DPK.

To sum up, the contribution of this paper can be summarized as follows:

- We propose the prior knowledge mechanism for feature distillation, which can fully excavates the distillation potential of big models. To the best of our knowledge, our method is the first to take the features of teachers as ‘input’, not just ‘target’.
- Based on our first contribution, we further propose the dynamic prior knowledge (DPK). Our DPK provides a solution to the ‘*larger models are not always better teachers*’ issue. Besides, it also gives better (or comparable) results under fair settings.

## 2 Methodology

In this section, we give the background of knowledge distillation, and then introduce the framework and details of our DPK.

### 2.1 Preliminary

The existing KD methods can be grouped into two categories. The logits-based KD methods distill the *dark knowledge* from the teacher by aligning the soft targets between the student and teacher, which can be formulated as a loss item:

$$\mathcal{L}_{logits} = \mathcal{D}_{logits}(\sigma(\mathbf{z}^s; \tau), \sigma(\mathbf{z}^t; \tau)), \quad (1)$$

where  $\mathbf{z}^s$  and  $\mathbf{z}^t$  are the logits from the student and the teacher.  $\sigma(\cdot)$  is the softmax function that produces the category probabilities from the logits, and  $\tau$  is a non-negative temperature hyper-

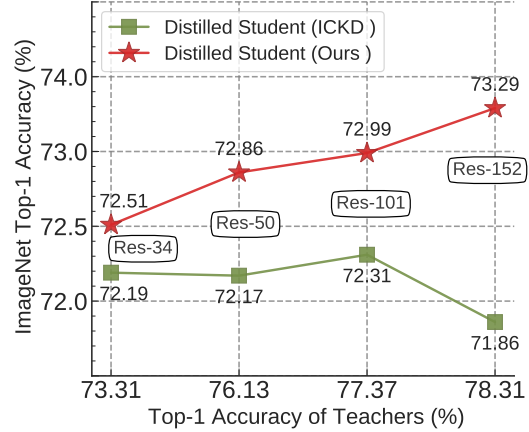


Figure 1: **Top-1 accuracy of ResNet-18 w.r.t. various teachers on ImageNet.** Different from the baseline (ICKD [34]), our method shows better performance and makes the performance of student positively correlated with that of the teacher.

parameter to scale the smoothness of predictive distribution. Specifically, we have  $\sigma_i(\mathbf{z}; \tau) = \text{softmax}(\exp(\mathbf{z}_i/\tau))$ .  $\mathcal{D}_{logits}$  is a loss function which can capture the difference between two categorical distributions, *e.g.* Kullback-Leibler divergence. Similarly, the feature-based KD methods, whose main idea is to mimic the feature representations between students and teachers, can also be represented as an auxiliary loss item:

$$\mathcal{L}_{feat} = \mathcal{D}_{feat}(\mathbf{T}_s(\mathbf{F}^s), \mathbf{T}_t(\mathbf{F}^t)), \quad (2)$$

where  $\mathbf{F}^s$  and  $\mathbf{F}^t$  denote the feature map from the student and the teacher, respectively.  $\mathbf{T}_s, \mathbf{T}_t$  denote the student and the teacher transformation module respectively, which align the dimensions of  $\mathbf{F}^s$  and  $\mathbf{F}^t$  (and transform the feature representations, such as [53]).  $\mathcal{D}_{feat}$  denotes the function which can compute the distance between two feature maps, such as  $\ell_1$ - or  $\ell_2$ -norm. So the KD methods can be represented by a generic paradigm. The final loss is the weighted sum of the classification loss  $\mathcal{L}_{cls}$  (the original training loss), the logits distillation loss, and the feature distillation loss:

$$\mathcal{L} = \mathcal{L}_{cls} + \alpha \mathcal{L}_{logits} + \beta \mathcal{L}_{feat}, \quad (3)$$

where  $\{\alpha, \beta\}$  are hyperparameters controlling the trade-off between these three losses.

## 2.2 Dynamic Prior Knowledge

An overview of the proposed DPK is presented in Fig. 2. As a feature distillation method, the main contributions of the DPK include the prior knowledge mechanism and dynamic mask generation. Here we give the details of these two designs.

**Prior knowledge.** To introduce the prior knowledge, the teacher provides part of its features to the student, and the Eq. 2 can be reformulated as:

$$\mathcal{L}_{feat} = \mathcal{D}_{feat}(\mathbf{T}_s(\mathbf{F}^s, \mathbf{F}^t), \mathbf{T}_t(\mathbf{F}^t)), \quad (4)$$

and then we introduce how to build the hybrid feature map, *i.e.* the student transformation module  $\mathbf{T}_s$ . Specifically, given the paired feature maps  $\mathbf{F}^s$  and  $\mathbf{F}^t$  from the student and the teacher, we divide them into several non-overlapping patches using a  $k \times k$  convolution with stride  $k$ , where  $k$  is the pre-defined size of the patches. Meanwhile, we also align the dimension of the features with this convolution layer. Then we randomly mask a subset of feature patches of the student under an uniform distribution with the ratio  $\pi$ , and also generate the complementary feature patches from the teachers. We take these feature patches as *token sequences* and use two ViT [14]-based encoders to further process them. After that, we stitch these token sequences together to generate the hybrid features (tokens), add the positional embedding to these hybrid tokens, and further integrate them with another ViT-based decoder. Finally, we re-organize generated token sequences into original shape and apply the feature distillation loss on the hybrid features and original teacher features. The transformation module  $\mathbf{T}_t$  for teacher feature is an identical mapping.

**Dynamic mechanism.** In the above solution, we mix the features of teacher and student with the hyper-parameter  $\pi$ . Furthermore, we empirically find that: (i) the optimal  $\pi$  for different model combinations is different, see Table 5 for related experiments, and (ii) the feature gap is different in the early and late stages of training phase. These facts inspire us to adjust the value of the masking ratio flexibly and dynamically according to the teacher-student gap, *e.g.* when the teacher-student gap is large, students need more prior knowledge to guide them. Formally, we set the iteration-specific masking ratio  $\pi$  at the  $i^{\text{th}}$  minibatch with the size of  $|\mathbf{B}|$  as:

$$\pi_i = 1 - \text{CKA}(\{\mathbf{F}_j^s\}_{j=1}^{|\mathbf{B}|}, \{\mathbf{F}_j^t\}_{j=1}^{|\mathbf{B}|}), \quad (5)$$

where the CKA [40] is the minibatch version of the Centered Kernel Alignment [27]. It is a representation similarity measure that is widely used for quantitative understanding the representations learned by neural networks. Particularly, CKA takes two sets of feature representations  $\mathbf{X}$  and  $\mathbf{Y}$  as input and computes their normalized similarity in terms of the Hilbert-Schmidt Independence Criterion (HSIC). CKA adopts an unbiased estimator of HSIC [49], *i.e.*  $\text{HSIC}_1$ , so that the value of CKA is independent of the batch size:

$$\text{HSIC}_1(\mathbf{K}, \mathbf{L}) = \frac{1}{n(n-3)} \left( \text{tr}(\tilde{\mathbf{K}}\tilde{\mathbf{L}}) + \frac{\mathbf{1}^\top \tilde{\mathbf{K}} \mathbf{1} \mathbf{1}^\top \tilde{\mathbf{L}} \mathbf{1}}{(n-1)(n-2)} - \frac{2}{n-2} \mathbf{1}^\top \tilde{\mathbf{K}} \tilde{\mathbf{L}} \mathbf{1} \right), \quad (6)$$

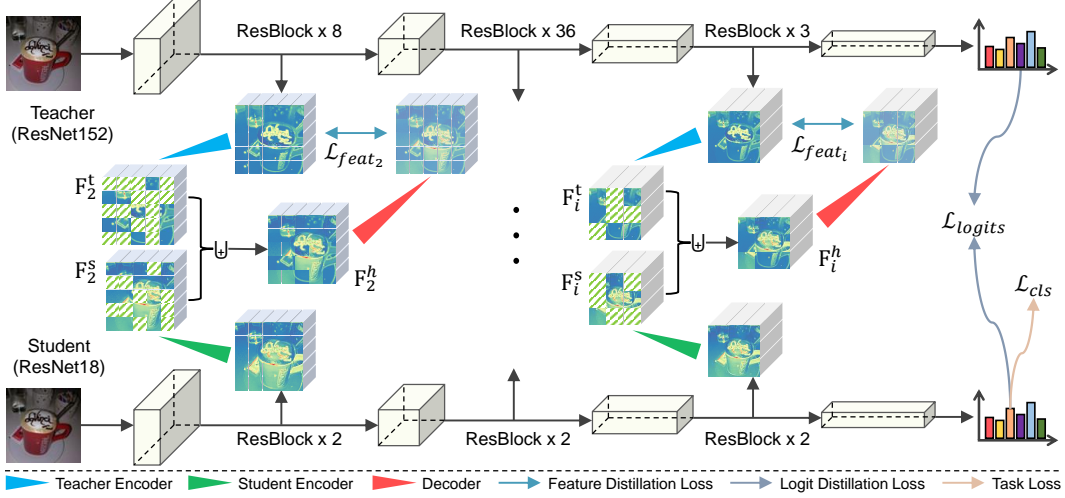


Figure 2: **Illustration of the proposed DPK.** For each feature distillation stage, the student feature map and the teacher feature map are sent to corresponding encoders to generate the  $F^s$  and  $F^t$ . Then, a subset of student feature patches is replaced by that of the teacher (the  $\oplus$  denotes the feature stitching operation). After that, DPK further integrate the hybrid feature  $F^h$  with a decoder before applying feature distillation loss. Note that the proportion of  $F^s$  and  $F^t$  in  $F^h$  is dynamically generated, which is omitted in this figure.

where  $\tilde{\mathbf{K}}$  and  $\tilde{\mathbf{L}}$  are obtained by setting the diagonal entries of similarity matrices  $\mathbf{K}$  and  $\mathbf{L}$  to zero. Then CKA is computed by averaging HISC<sub>1</sub> scores over  $k$  minibatches:

$$\text{CKA} = \frac{\frac{1}{k} \sum_{i=1}^k \text{HISC}_1(\mathbf{X}_i \mathbf{X}_i^T, \mathbf{Y}_i \mathbf{Y}_i^T)}{\sqrt{\frac{1}{k} \sum_{i=1}^k \text{HISC}_1(\mathbf{X}_i \mathbf{X}_i^T, \mathbf{X}_i \mathbf{X}_i^T)} \sqrt{\frac{1}{k} \sum_{i=1}^k \text{HISC}_1(\mathbf{Y}_i \mathbf{Y}_i^T, \mathbf{Y}_i \mathbf{Y}_i^T)}}, \quad (7)$$

where  $\mathbf{X}_i \in \mathbb{R}^{|\mathcal{B}| \times p_1}$  and  $\mathbf{Y}_i \in \mathbb{R}^{|\mathcal{B}| \times p_2}$  are now matrices containing activations of the  $i^{\text{th}}$  minibatch of  $|\mathcal{B}|$  examples. Given a minibatch of teacher and student feature sets, we flatten them, yielding  $\mathbf{F}_t \in \mathbb{R}^{|\mathcal{B}| \times c \times h \times w} \mapsto \mathbf{X} \in \mathbb{R}^{|\mathcal{B}| \times p_1}$  and  $\mathbf{F}_s \in \mathbb{R}^{|\mathcal{B}| \times c \times h \times w} \mapsto \mathbf{Y} \in \mathbb{R}^{|\mathcal{B}| \times p_2}$ .

Due to the space limitation, we only introduce the main designs of our DPK, and more implementation details can be found in Appendix A.1.

### 3 Experiments

We conduct extensive experiments on *image classification* and *object detection*. Moreover, we present various *ablations* and *analysis* for the proposed method. Besides, our codes will be publicly available for the reproducibility.

#### 3.1 Image Classification

We evaluate our method on **CIFAR-100** [28] and **ImageNet** [12] for image classification. CIFAR-100 contains 50K images for training and 10K images for testing, labeled into 100 fine-grained categories. The size of each image is  $32 \times 32$ . We evaluate the proposed DPK on this dataset with image recognition and report the top-1 accuracy. ImageNet [12] consists of 1.2M images for training and 50K images for validation, covering 1,000 categories. All images are resized to  $224 \times 224$  during training and testing. We report the top-1 and top-5 accuracy on this dataset for image recognition.

**Results on CIFAR-100.** We first evaluate DPK on the CIFAR-100 dataset and summarize the results on Table 1. From these results, we can observe that the proposed DPK performs best for all six teacher-student pairs (more experiments for other network combinations can be found in Appendix A.2), which firmly demonstrates the effectiveness of our method.

**Results on ImageNet.** We also conduct experiments on the large-scale ImageNet to evaluate our DPK. In particular, following the previous conventions [52, 7], we present the performance of ResNet-

Table 1: **Results on the CIFAR-100 validation set.** We report the top-1 accuracy (%) of the methods for *homogeneous* teacher-student pairs. “-” indicates results are not available, and we highlight the best results in **bold**.

Teacher	WRN40-2	WRN40-2	ResNet56	ResNet110	ResNet110	VGG13
Acc.	75.61	75.61	72.34	74.31	74.31	74.64
Student	WRN16-2	WRN40-1	ResNet20	ResNet20	ResNet32	VGG8
Acc.	73.26	71.98	69.06	69.06	71.14	70.36
KD [22]	74.92	73.54	70.66	70.67	73.08	72.98
FitNets [48]	73.58	72.24	69.21	68.99	71.06	71.02
AT [63]	74.08	72.77	70.55	70.22	72.31	71.43
PKT [42]	74.54	73.45	70.34	70.25	72.61	72.88
SP [53]	73.83	72.43	69.67	70.04	72.69	72.68
CC [44]	73.56	72.21	69.63	69.48	71.48	70.71
RKD [41]	73.35	72.22	69.61	69.25	71.82	71.48
VID [1]	74.11	73.30	70.38	70.16	72.61	71.23
CRD [52]	75.48	74.14	71.16	71.46	73.48	73.94
OFD [20]	75.24	74.33	70.98	-	73.23	73.95
ReviewKD [7]	76.12	75.09	71.89	-	73.89	74.84
DKD [65]	76.24	74.81	71.97	-	74.11	74.68
ICKD-C [34]	75.57	74.63	71.69	71.91	74.11	73.88
<b>DTKA</b>	<b>76.42</b>	<b>75.27</b>	<b>72.37</b>	<b>72.28</b>	<b>74.89</b>	<b>74.96</b>

Table 2: **Results on ImageNet validation set.** We show the top-1 and top-5 accuracy (%) for ResNet18 guided by ResNet34. “-” indicates the results are not available.

Acc.	Student	Teacher	KD [22]	RKD [41]	CRD+KD [52]	SAD [24]	CC [44]	ICKD-C [34]	ReviewKD [7]	DKD [65]	Ours
Top-1	69.55	73.31	70.68	71.34	71.38	71.38	70.74	72.19	71.61	71.70	<b>72.51</b>
Top-5	89.09	91.42	90.16	90.37	-	90.49	-	90.72	90.51	90.41	<b>90.77</b>

Table 3: **Results for heterogeneous models.** We show the top-1 and top-5 accuracy (%) of MobileNetV2 guided by ResNet50 on ImageNet validation set.

Acc.	Student	Teacher	FT [26]	AB [21]	AT [63]	OFD [20]	CRD [52]	ReviewKD [7]	KD [22]	DKD [65]	Ours
Top-1	68.87	76.16	69.88	69.89	69.56	71.25	71.37	72.56	68.58	72.05	<b>73.26</b>
Top-5	88.76	92.86	89.50	88.71	89.33	90.34	90.41	91.00	88.98	91.05	<b>91.17</b>

18 guided by ResNet-34 in Table 2. The results show the superiority of DPK in performance to other baselines. Note that our method still works for other teacher-student combinations, and see Appendix A.2 for the related experiments.

**KD for heterogeneous models.** Table 1 and 2 show the experiments for homogeneous models (*e.g.* ResNet18 and ResNet34), and we show our method can also be applied to heterogeneous models (*e.g.* MobileNet and ResNet50) in this part. From the results shown in Table 3, we can find DPK performs best among all listed methods for heterogeneous models (more experiments for this setting can be found in Appendix A.3).

**Better teacher, better student.** The above experiments show DPK performs well for the common teacher-student pairs. Here we show our method can be further improved with better teachers. As illustrated in Fig. 3, the accuracy of the student model trained by our method is continuously improved by progressively replacing larger teacher models, while the model trained by other algorithms fluctuates in performance. Meanwhile, our method surpasses its counterparts at each stage and progressively widens the performance gap. To show the generalization, we also present the performance change for other teacher-student combinations in Fig. 4, which confirms the same conclusion again. Note that it is a reasonable phenomenon that the performance of the given student tends to be saturated gradually, but the performance fluctuation will bring many difficulties to the practical applications.

### 3.2 Object Detection

DPK can also be applied to other tasks, and we evaluate it on a popular one, *i.e.* object detection. Note that our method can be easily integrated into other KD methods, and we apply DPK into FGD [59] and evaluate the performance on the most commonly used MS-COCO dataset [31]. MS-COCO

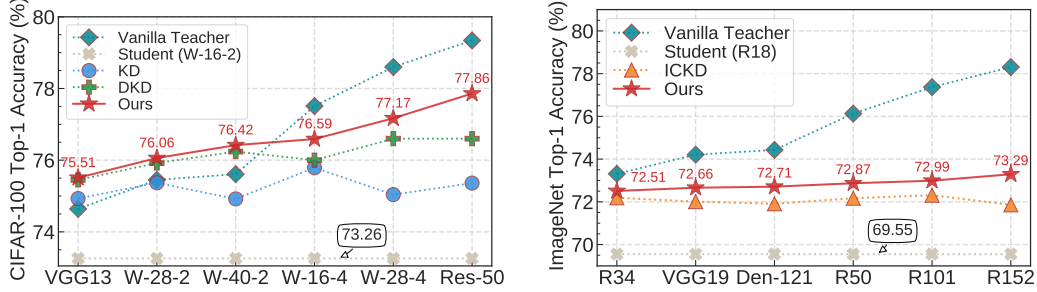


Figure 3: **Better teacher, better student.** We show the top-1 accuracy of our method and some baselines on the CIFAR-100 (left) and ImageNet (right).

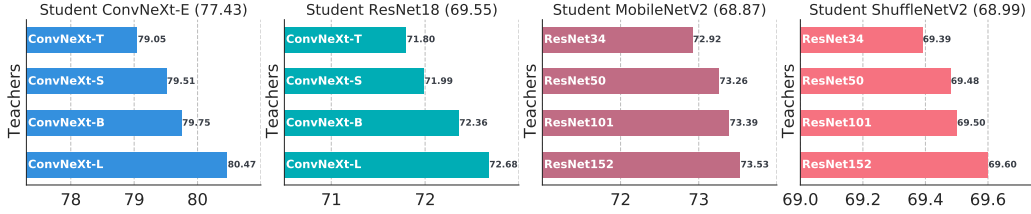


Figure 4: **More teacher-student combinations**, covering the lightweight ShuffleNetV2 [38] to the recently ConvNeXt [37]. Top-1 accuracy (%) on ImageNet val set is reported. Both *homogeneous* and *heterogeneous* settings are considered. By changing the teacher size, we see that, *larger models are always better teachers* for our method. ConvNeXt-E is a small model build by us following the design principles of [37], see Appendix A.1 for details. Best viewed in color with zoom in.

[31] is the most commonly used object detection benchmark, which contains 80 categories. We also conduct experiments for object detection to further evaluate our DPK. In particular, we use `train2017` (118K images) for training, and test on `val2017` (5K images). We adopt the standard evaluation protocol introduced by COCO, *e.g.* mAP, AP<sub>50</sub>, AP<sub>75</sub>, *etc.*

**Comparison with SOTA methods.** As presented in Table 4, we evaluate our model on a one-stage detector (RetinaNet [33]) and a two-stage detector (Faster-RCNN [47]) with several strong baselines [56, 11, 15, 59]. Following the previous conventions, we first adopt the ResNet101-FPN as the teacher model and ResNet50-FPN as the student model, and our model achieves better performance than other baselines, *i.e.* surpassing the recently published FGD [59] by 0.1/0.2 mAP with RetinaNet/Faster RCNN frameworks.

**Better teacher, better student.** Similar to image classification, our method also benefits from better teacher model for object detection. In particular, we enlarge the capacity gap between the teacher and student models, and the results in Table 4 suggest that effectiveness of our method can be further improved by replacing more powerful teacher models. For instance, replacing teacher model from ResNet101-FPN to ResNet152-FPN further improves the student’s performance (ResNet50-FPN, Faster RCNN) by 0.6 mAP, while the number for FGD [59] is 0.1 for the same setting. This conclusion also stands for other teacher-student pairs and frameworks.

### 3.3 Ablation Studies

In this section, we provide extensive ablation studies to analyze the effects of each component of DPK. The experiments are conducted on ImageNet for classification task, ResNet34 and ResNet18 are adopted as teacher and student and last stage distillation unless stated otherwise.

**Masking ratio.** Features masking (and stitching) is a key component of our method, and Table 5 reports the results of various DPK variants under different masking ratios. For fair comparison, we only distill the features of the last stage among all teacher-student transfer pairs. Note that when the masking rate is set to 0, our model reduces to the traditional feature distillation scheme. Surprisingly, a *broad* range of masking ratios from 15% to 95% can offer considerable performance gains for students. This implies that the prior knowledge provided by teachers is very beneficial to students’

Table 4: **Results on object detection.** Experiments are evaluated on COCO validation set. ‘T’ and ‘S’ represent the teacher and the student, respectively. ‘-’ indicates results are not available.

Methods	RetinaNet						Faster-RCNN					
	mAP	AP <sub>50</sub>	AP <sub>75</sub>	AP <sub>S</sub>	AP <sub>M</sub>	AP <sub>L</sub>	mAP	AP <sub>50</sub>	AP <sub>75</sub>	AP <sub>S</sub>	AP <sub>M</sub>	AP <sub>L</sub>
R101-FPN(T)	38.9	58.0	41.5	21.0	42.8	52.4	39.9	60.1	43.3	23.5	44.2	51.5
R50-FPN(S)	37.4	56.7	39.6	20.6	40.7	49.7	38.4	59.0	42.0	21.5	42.1	50.3
FGFI [56]	38.6	58.7	41.3	21.4	42.5	51.5	39.3	59.8	42.9	22.5	42.3	52.2
GID [11]	39.1	59.0	42.3	22.8	43.1	52.3	40.2	60.7	43.8	22.7	44.0	53.2
FGD [59]	39.6	-	-	22.9	43.7	53.6	40.4	-	-	22.8	44.5	53.5
Ours	<b>39.7</b>	58.6	42.5	22.8	43.6	53.6	<b>40.6</b>	60.7	44.4	22.8	44.7	54.0
R152-FPN(T)	39.9	59.4	42.7	23.5	44.2	51.5	41.6	62.3	45.4	23.3	46.1	53.6
R50-FPN(S)	37.4	56.7	39.6	20.6	40.7	49.7	38.4	59.0	42.0	21.5	42.1	50.3
FGFI [56]	38.9	-	-	21.9	42.5	52.2	39.9	-	-	22.9	43.6	52.8
DeFeat [15]	39.7	-	-	23.4	43.6	52.9	40.9	-	-	23.6	44.8	53.5
FGD [59]	39.7	58.9	42.9	23.2	44.0	52.7	40.5	61.1	44.2	23.4	44.4	53.7
Ours	<b>40.2</b>	59.6	43.0	23.4	44.5	53.6	<b>41.2</b>	61.6	45.0	23.3	45.2	54.3
R101-FPN(T)	38.9	58.0	41.5	21.0	42.8	52.4	39.9	60.1	43.3	23.5	44.2	51.5
R18-FPN(S)	33.1	51.4	34.9	17.4	35.8	43.4	33.8	53.2	36.8	19.2	36.6	43.6
FGD [59]	34.7	52.5	37.1	17.8	38.0	48.5	36.0	55.8	39.2	18.3	39.4	48.7
Ours	<b>35.8</b>	53.9	38.2	19.1	39.4	49.1	<b>36.7</b>	56.2	40.1	19.2	40.3	49.2

network learning. Besides, note that the optimal mask ratio is *inconsistent* under different teacher-student pairs. This suggests the necessity of a *dynamic masking strategy* for automatic selection of masking ratios depending on the teacher-student pairs. Table 5 shows that students achieve the best (or comparable) accuracy using the proposed dynamic masking strategy, revealing its effectiveness.

Table 5: **Ablations on mask ratios.** We report the accuracy on ImageNet with setting (a): ResNet18 as student, ResNet34 as teacher, and setting (b): ResNet18 as student, ResNet101 as teacher.

setting	acc.	teacher	student	0%	15%	35%	55%	75%	95%	dynamic
(a)	Top-1	73.31	69.55	72.01	72.33	72.34	<b>72.38</b>	72.36	72.34	<b>72.46</b>
	Top-5	91.42	89.09	90.40	90.62	90.59	<b>90.69</b>	90.61	90.59	<b>90.67</b>
(b)	Top-1	77.37	69.55	72.25	72.46	72.55	72.57	<b>72.60</b>	72.53	<b>72.87</b>
	Top-5	93.55	89.09	90.66	90.73	<b>90.77</b>	<b>90.77</b>	90.75	90.75	<b>90.96</b>

**Masking strategy.** In Table 6 we summarize the effects of different masking strategies. ResNet34 and ResNet18 are adopted as teacher and student for all experiments in this part. For the fixed masking ratio, we take the sample random masking as baseline, and consider the `block-wise` masking strategy, introduced by BEIT [2]. We also consider `grid-wise` masking, which regularly retains one of every four patches, similar to MAE [17]. Beyond a fixed masking ratio, several alternatives for realizing a dynamic masking ratio are explored. Particularly, the `cosinesimi` indicates that we use the cosine similarity to measure the teacher-student feature gap. The `exponential` decay schedule divides the masking ratio by the same factor every epoch, which can be expressed as  $\pi_i = \pi_0 * (0.95)^{\text{epoch}_i}$ , where  $\pi_0$  is the initial masking ratio and is set to 1.0. The `linear` schedule decreases the masking ratio by the same decrement every epoch, which is defined as  $\pi_i = \pi_0 - (\text{epoch}_i * \text{decrement})$ , and we set `decrement` = 0.95. The results reveal that: *i*) simple random sampling works best for our DPK when using fixed masking ratios. *ii*) 1-CKA outperforms its competitors, and we use it to yield dynamic masking ratios by default.

**Prior knowledge.** Table 7 ablates the importance of integrating teacher’s knowledge in building the hybrid student feature map (Eq. 4). Specifically, we use `zero-padding` or `learnable` mask token to take the role of teacher’s feature in the masked position. The token vector dimension is set to the same as that of the other visible patch representations. It’s shown that no prior knowledge provided by the teacher leads to worse performance, as it aggravates the burden of feature imitation from students to teachers. This confirms the effectiveness of offering students the prior knowledge from the teacher.

Table 6: **Ablations on masking strategies.**

Masking Strategy	Ratio	Top-1	Top-5
Vanilla	$\times$	69.55	89.09
Random	75%	72.36	90.61
Block-wise	75%	72.36	90.57
Grid-wise	75%	72.32	90.38
1-CKA	$\times$	<b>72.46</b>	<b>90.67</b>
1-CosineSimi	$\times$	72.38	90.58
Exponential decay	$\times$	72.35	90.51
Linear decay	$\times$	72.36	90.58

Table 7: **Ablations on prior knowledge.**

Prior Knowledge	Top-1	Top-5
Zero-padding	72.16	90.35
Learnable	72.28	90.63
T-knowledge	<b>72.46</b>	<b>90.67</b>

Table 8: **Ablations on transformation functions.**

Transform	Top-1	Top-5
FitNets [48]	71.08	90.00
Conv	71.39	90.46
Decoder	72.31	90.50
Encoder-Decoder	<b>72.46</b>	<b>90.67</b>

Table 9: **Ablations on loss calculation.**

Target	Top-1	Top-5
Masked	72.39	90.63
Full	<b>72.46</b>	<b>90.67</b>

**Transformation module.** For feature-based distillation methods, a teacher transform module  $T_t$  is required to convert its features into an easy-to-transfer form [20], while a student transform module  $T_s$  adopts the same function as  $T_t$ . We take FitNets [48] as the baseline, which does not reduce the dimension of teacher’s feature map and use a  $1 \times 1$  convolutional layer as the student transformation to match the feature dimension of the student to that of the teacher. Our transformation modules convert both the teacher’s and student’s features to make them dimensionally aligned, similar to FT [26]. To this end, we carefully design three transform modules, namely `encoder-decoder`, `decoder` and `conv`. The implementation details are deferred to the Appendix A.1. Table 8 shows the results, and we can observe that `encoder-decoder` reaches best performance and is therefore the default transformation.

**Loss calculation.** We train the network by computing the mean squared error (MSE) between the reconstructed teacher features and the original teacher features in Eq. 4, where the loss can be computed between only the masked teacher features, namely `masked`, or between all features, namely `full`. Table 9 shows the ablation results for these two settings. The results show that computing the loss on the full feature performs better.

**Multi-stage distillation.** Finally, we study the effect of multi-stage feature distillation in DPK. As listed in Table 10, we apply the feature mimicking losses at the last stage (stage 4), the last two stages (stage 3&4), and the last three stages (stage 2&3&4) respectively, where the same masking strategy is applied at each stage. We report the best-performing results among these distillation stage compositions in the following experiments. Overall, multi-stage distillation performs better than single-stage distillation, and the last two stage distillation works best in most cases. We adopt stage 3&4 distillation as default setting in all experiments.

Table 10: **Ablations on multi-stage distillation.** We adopt ResNet18 as student model.

Teacher	Acc.	Stage 4	Stage 3&4	Stage 2&3&4
ResNet34	Top-1	72.46	<b>72.51</b>	72.45
	Top-5	90.67	<b>90.77</b>	90.55
ResNet50	Top-1	72.65	<b>72.87</b>	72.82
	Top-5	90.65	<b>90.92</b>	90.83
ResNet101	Top-1	72.87	72.99	<b>73.00</b>
	Top-5	90.96	90.94	<b>91.03</b>
ResNet152	Top-1	72.74	<b>73.29</b>	73.09
	Top-5	90.91	<b>91.10</b>	90.95

### 3.4 Visualizations

In this part, we present some visualizations to show that our DPK does bridge the teacher-student gap in the feature-level. In particular, we visualize the feature similarity between ResNet18 and ResNet34 (see Appendix A.5 for more teacher-student combinations) in Fig. 5. We can find that our DPK significantly improves the feature similarity (measured by CKA) between the student and the teacher. ICKD gets a lower similarity than the baseline, which may be because it models the feature relationships, instead of the features themselves. Besides, the CKA curve in the training phase can also be found in Appendix A.5.

## 4 Related Work

**Knowledge Distillation.** Existing studies on knowledge distillation (KD) can be roughly categorized into two groups, *logits-based* distillation and *feature-based* distillation. **The former**, pioneered by [22], is known as the classical KD, aiming to learn a compact student by mimicking the softmax outputs (logits) of an over-parameterized teacher. This line of work focuses on proposing effective regularization and optimization techniques [64]. Recently, DKD [65] proposes to decouple the classical KD loss into two parts, *i.e.*, target class KD and non-target KD. Besides, several works [45, 8]

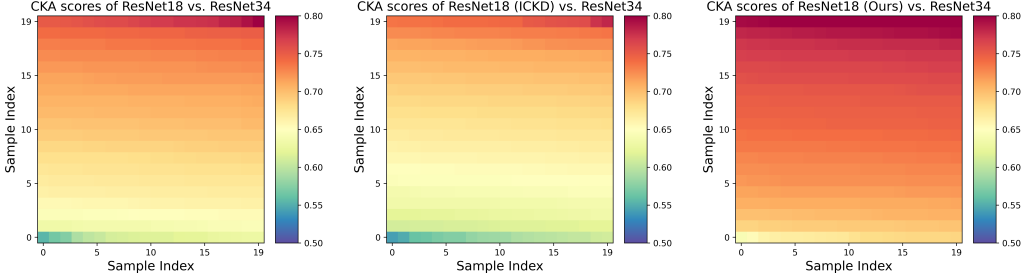


Figure 5: **CKA similarity between ResNet18 and ResNet34.** We visualize the CKA similarity (the larger the value, the more similar the features are) of the original models (*left*), the models trained by ICKD (*middle*), and the models trained by our DPK (*right*). The experiments are conducted on the sampled ImageNet validation set (12,800 samples). We compute CKA with a batchsize of 32 for the last stage, so these are 400 CKA values for each experiment. For better presentation, we rank these values and organize them as the heatmap representation.

also attempt to interpret the classical KD. **The latter**, represented by FitNet [48], encourages students to mimic the intermediate-level features (*hints*) from the hidden layers of teacher models. Since features are more informative than logits, feature-based distillation methods usually perform better than logits-based ones in the tasks that involve the localization information, such as object detection [30, 56, 11, 15, 59]. This line of work mainly investigates what kinds of intermediate representations of features should be. These representations include singular value decomposition [29], attention maps [63], Gramian matrices [60], gradients [50], pre-activations [21], similarities and dissimilarities [53], instance relationships [36, 41], inter-channel correlations [34] and inter-region affinity [23]. Besides, the research interests in this direction also cover channel matching [62], distance function design [20] and semantic calibration [63, 5, 24] between teachers and students.

Among these works, [9, 39, 22, 34] also report that the performance of distilled student *degrades* when the gap between students and teachers becomes *large*. To solve this issue, ESKD [9] stops the teacher training early to make it under convergence and yield more softened logits. TAKD [39] introduces an extra intermediate-sized network termed *teacher assistant* to bridge the gap between teachers and students. Different from the above logits-based methods, DPK directly reduces the gap between teachers and students in the feature space, unleashing the full potential of large teachers.

**Masked Image Modeling.** Emerged with the masked language modeling in NLP community, such as BERT [13] and GPT [46, 3], masked image modeling (MIM) [43, 19] has gained increasing attention and shows promising potentials in representation learning. Particularly, MIM-based approaches generally *i)* divide an image or video into several non-overlapping patches or discrete visual tokens, *ii)* mask random subsets of these patches/tokens, and *iii)* predict the patches masked visual tokens [2], the feature of the masked regions such as HOG [57], or reconstruct the masked pixels [17, 58]. In contrast to these approaches, our masking strategy operates on feature maps between students and teachers with the aim of narrowing the feature gap between them. Our masking ratio is dynamic, dependent on the teacher-student feature gap. Moreover, instead of replacing the masked regions with [MASK] tokens [17, 58], we use the feature patches of teachers to fill the masked regions of students, thereby making our distillation teacher knowledge-aware.

## 5 Conclusion

In this paper, we demonstrate the potential of masked feature prediction in mining richer knowledge from teacher networks. In particular, we design a prior knowledge-aware feature distillation method, named DPK, and tailor a dynamic masking ratio scheme to dynamically regulate the training process by capturing the feature gap between teacher-student pairs. Extensive experiments show that our knowledge distillation method achieves state-of-the-art performance on several commonly-used benchmarks (*i.e.*, CIFAR100, ImageNet, and MS COCO) under various settings. More importantly, our DPK allows students’ accuracy to be positively correlated with that of the teacher. This feature of our model further boosts the performance of students and provides a “shortcut” for teacher selection.

## References

- [1] Sungsoo Ahn, Shell Xu Hu, Andreas C. Damianou, Neil D. Lawrence, and Zhenwen Dai. Variational information distillation for knowledge transfer. In *CVPR*, 2019.
- [2] Hangbo Bao, Li Dong, and Furu Wei. Beit: Bert pre-training of image transformers. In *ICLR*, 2022.
- [3] Tom Brown, Benjamin Mann, Nick Ryder, Melanie Subbiah, Jared D Kaplan, Prafulla Dhariwal, Arvind Neelakantan, Pranav Shyam, Girish Sastry, Amanda Askell, et al. Language models are few-shot learners. In *NeurIPS*, 2020.
- [4] Cristian Bucilua, Rich Caruana, and Alexandru Niculescu-Mizil. Model compression. In *KDD*, 2006.
- [5] Defang Chen, Jian-Ping Mei, Yeliang Zhang, Can Wang, Zhe Wang, Yan Feng, and Chun Chen. Cross-layer distillation with semantic calibration. In *AAAI*, 2021.
- [6] Kai Chen, Jiaqi Wang, Jiangmiao Pang, Yuhang Cao, Yu Xiong, Xiaoxiao Li, Shuyang Sun, Wansen Feng, Ziwei Liu, Jiarui Xu, Zheng Zhang, Dazhi Cheng, Chenchen Zhu, Tianheng Cheng, Qijie Zhao, Buyu Li, Xin Lu, Rui Zhu, Yue Wu, Jifeng Dai, Jingdong Wang, Jianping Shi, Wanli Ouyang, Chen Change Loy, and Dahua Lin. MMDetection: Open mmlab detection toolbox and benchmark. *arXiv*, abs/1906.07155, 2019.
- [7] Pengguang Chen, Shu Liu, Hengshuang Zhao, and Jiaya Jia. Distilling knowledge via knowledge review. In *CVPR*, 2021.
- [8] Xu Cheng, Zhefan Rao, Yilan Chen, and Quanshi Zhang. Explaining knowledge distillation by quantifying the knowledge. In *CVPR*, 2020.
- [9] Jang Hyun Cho and Bharath Hariharan. On the efficacy of knowledge distillation. In *ICCV*, 2019.
- [10] Zhiyu Chong, Xinzhu Ma, Hong Zhang, Yuxin Yue, Haojie Li, Zhihui Wang, and Wanli Ouyang. Monodistill: Learning spatial features for monocular 3d object detection. In *ICLR*, 2022.
- [11] Xing Dai, Zeren Jiang, Zhao Wu, Yiping Bao, Zhicheng Wang, Si Liu, and Erjin Zhou. General instance distillation for object detection. In *CVPR*, 2021.
- [12] Jia Deng, Wei Dong, Richard Socher, Li-Jia Li, Kai Li, and Li Fei-Fei. Imagenet: A large-scale hierarchical image database. In *CVPR*, 2009.
- [13] Jacob Devlin, Ming-Wei Chang, Kenton Lee, and Kristina Toutanova. Bert: Pre-training of deep bidirectional transformers for language understanding. *arXiv*, abs/1810.04805, 2018.
- [14] Alexey Dosovitskiy, Lucas Beyer, Alexander Kolesnikov, Dirk Weissenborn, Xiaohua Zhai, Thomas Unterthiner, Mostafa Dehghani, Matthias Minderer, Georg Heigold, Sylvain Gelly, et al. An image is worth 16x16 words: Transformers for image recognition at scale. In *ICLR*, 2020.
- [15] Jianyuan Guo, Kai Han, Yunhe Wang, Han Wu, Xinghao Chen, Chunjing Xu, and Chang Xu. Distilling object detectors via decoupled features. In *CVPR*, 2021.
- [16] Hai Victor Habi, Roy H Jennings, and Arnon Netzer. Hmq: Hardware friendly mixed precision quantization block for cnns. In *ECCV*, 2020.
- [17] Kaiming He, Xinlei Chen, Saining Xie, Yanghao Li, Piotr Dollár, and Ross Girshick. Masked autoencoders are scalable vision learners. In *CVPR*, 2021.
- [18] Yihui He, Xiangyu Zhang, and Jian Sun. Channel pruning for accelerating very deep neural networks. In *ICCV*, 2017.
- [19] Olivier Henaff. Data-efficient image recognition with contrastive predictive coding. In *ICML*, 2020.
- [20] Byeongho Heo, Jeessoo Kim, Sangdoo Yun, Hyojin Park, Nojun Kwak, and Jin Young Choi. A comprehensive overhaul of feature distillation. In *ICCV*, 2019.

- [21] Byeongho Heo, Minsik Lee, Sangdoo Yun, and Jin Young Choi. Knowledge transfer via distillation of activation boundaries formed by hidden neurons. In *AAAI*, 2019.
- [22] Geoffrey E. Hinton, Oriol Vinyals, and J. Dean. Distilling the knowledge in a neural network. *ArXiv*, abs/1503.02531, 2015.
- [23] Yuenan Hou, Zheng Ma, Chunxiao Liu, Tak-Wai Hui, and Chen Change Loy. Inter-region affinity distillation for road marking segmentation. In *CVPR*, 2020.
- [24] Mingi Ji, Byeongho Heo, and S. Park. Show, attend and distill: Knowledge distillation via attention-based feature matching. In *AAAI*, 2021.
- [25] Alex Kendall and Yarin Gal. What uncertainties do we need in bayesian deep learning for computer vision? In *NeurIPS*, 2017.
- [26] Jangho Kim, SeongUk Park, and Nojun Kwak. Paraphrasing complex network: Network compression via factor transfer. In *NeurIPS*, 2018.
- [27] Simon Kornblith, Mohammad Norouzi, Honglak Lee, and Geoffrey Hinton. Similarity of neural network representations revisited. In *ICML*, 2019.
- [28] Alex Krizhevsky, Geoffrey Hinton, et al. *Learning multiple layers of features from tiny images*. Citeseer, 2009.
- [29] Seung Hyun Lee, Dae Ha Kim, and Byung Cheol Song. Self-supervised knowledge distillation using singular value decomposition. In *ECCV*, 2018.
- [30] Quanquan Li, Shengying Jin, and Junjie Yan. Mimicking very efficient network for object detection. In *CVPR*, 2017.
- [31] Tsung-Yi Lin, Michael Maire, Serge Belongie, James Hays, Pietro Perona, Deva Ramanan, Piotr Dollár, and C Lawrence Zitnick. Microsoft coco: Common objects in context. In *ECCV*, 2014.
- [32] Tsung-Yi Lin, Piotr Dollár, Ross Girshick, Kaiming He, Bharath Hariharan, and Serge Belongie. Feature pyramid networks for object detection. In *CVPR*, 2017.
- [33] Tsung-Yi Lin, Priya Goyal, Ross Girshick, Kaiming He, and Piotr Dollár. Focal loss for dense object detection. In *ICCV*, 2017.
- [34] Li Liu, Qingle Huang, Sihao Lin, Hongwei Xie, Bing Wang, Xiaojun Chang, and Xiaodan Liang. Exploring inter-channel correlation for diversity-preserved knowledge distillation. In *ICCV*, 2021.
- [35] Yifan Liu, Ke Chen, Chris Liu, Zengchang Qin, Zhenbo Luo, and Jingdong Wang. Structured knowledge distillation for semantic segmentation. In *CVPR*, 2019.
- [36] Yufan Liu, Jiajiong Cao, Bing Li, Chunfeng Yuan, Weiming Hu, Yangxi Li, and Yunqiang Duan. Knowledge distillation via instance relationship graph. In *CVPR*, 2019.
- [37] Zhuang Liu, Hanzi Mao, Chao-Yuan Wu, Christoph Feichtenhofer, Trevor Darrell, and Saining Xie. A convnet for the 2020s. In *CVPR*, 2022.
- [38] Ningning Ma, Xiangyu Zhang, Hai-Tao Zheng, and Jian Sun. Shufflenet v2: Practical guidelines for efficient cnn architecture design. In *ECCV*, 2018.
- [39] Seyed Iman Mirzadeh, Mehrdad Farajtabar, Ang Li, Nir Levine, Akihiro Matsukawa, and Hassan Ghasemzadeh. Improved knowledge distillation via teacher assistant. In *AAAI*, 2020.
- [40] Thao Nguyen, Maithra Raghu, and Simon Kornblith. Do wide and deep networks learn the same things? uncovering how neural network representations vary with width and depth. In *ICLR*, 2020.
- [41] Wonpyo Park, Dongju Kim, Yan Lu, and Minsu Cho. Relational knowledge distillation. In *CVPR*, 2019.

- [42] N. Passalis and A. Tefas. Learning deep representations with probabilistic knowledge transfer. In *ECCV*, 2018.
- [43] Deepak Pathak, Philipp Krahenbuhl, Jeff Donahue, Trevor Darrell, and Alexei A Efros. Context encoders: Feature learning by inpainting. In *CVPR*, 2016.
- [44] Baoyun Peng, Xiao Jin, Jiaheng Liu, Dongsheng Li, Yichao Wu, Yu Liu, Shunfeng Zhou, and Zhaoning Zhang. Correlation congruence for knowledge distillation. In *ICCV*, 2019.
- [45] Mary Phuong and Christoph Lampert. Towards understanding knowledge distillation. In *ICML*, 2019.
- [46] Alec Radford, Jeffrey Wu, Rewon Child, David Luan, Dario Amodei, Ilya Sutskever, et al. Language models are unsupervised multitask learners. *OpenAI blog*, 2019.
- [47] Shaoqing Ren, Kaiming He, Ross Girshick, and Jian Sun. Faster r-cnn: Towards real-time object detection with region proposal networks. In *NeurIPS*, 2015.
- [48] A. Romero, Nicolas Ballas, S. Kahou, Antoine Chassang, C. Gatta, and Yoshua Bengio. Fitnets: Hints for thin deep nets. In *ICLR*, 2015.
- [49] Le Song, Alex Smola, Arthur Gretton, Justin Bedo, and Karsten Borgwardt. Feature selection via dependence maximization. In *JMLR*, 2012.
- [50] Suraj Srinivas and François Fleuret. Knowledge transfer with jacobian matching. In *ICML*, 2018.
- [51] Mingxing Tan and Quoc Le. Efficientnet: Rethinking model scaling for convolutional neural networks. In *ICML*, 2019.
- [52] Yonglong Tian, Dilip Krishnan, and Phillip Isola. Contrastive representation distillation. In *ICLR*, 2020.
- [53] F. Tung and G. Mori. Similarity-preserving knowledge distillation. In *ICCV*, 2019.
- [54] Ashish Vaswani, Noam Shazeer, Niki Parmar, Jakob Uszkoreit, Llion Jones, Aidan N Gomez, Łukasz Kaiser, and Illia Polosukhin. Attention is all you need. In *NeurIPS*, 2017.
- [55] Alvin Wan, Xiaoliang Dai, Peizhao Zhang, Zijian He, Yuandong Tian, Saining Xie, Bichen Wu, Matthew Yu, Tao Xu, Kan Chen, et al. Fbnetv2: Differentiable neural architecture search for spatial and channel dimensions. In *CVPR*, 2020.
- [56] Tao Wang, Li Yuan, Xiaopeng Zhang, and Jiashi Feng. Distilling object detectors with fine-grained feature imitation. In *CVPR*, 2019.
- [57] Chen Wei, Haoqi Fan, Saining Xie, Chao-Yuan Wu, Alan Yuille, and Christoph Feichtenhofer. Masked feature prediction for self-supervised visual pre-training. *arXiv preprint arXiv:2112.09133*, 2021.
- [58] Zhenda Xie, Zheng Zhang, Yue Cao, Yutong Lin, Jianmin Bao, Zhuliang Yao, Qi Dai, and Han Hu. Simmim: A simple framework for masked image modeling. In *CVPR*, 2021.
- [59] Zhendong Yang, Zhe Li, Xiaohu Jiang, Yuan Gong, Zehuan Yuan, Danpei Zhao, and Chun Yuan. Focal and global knowledge distillation for detectors. In *CVPR*, 2022.
- [60] Junho Yim, Donggyu Joo, Jihoon Bae, and Junmo Kim. A gift from knowledge distillation: Fast optimization, network minimization and transfer learning. In *CVPR*, 2017.
- [61] Junho Yim, Donggyu Joo, Jihoon Bae, and Junmo Kim. A gift from knowledge distillation: Fast optimization, network minimization and transfer learning. In *CVPR*, 2017.
- [62] Kaiyu Yue, Jiangfan Deng, and Feng Zhou. Matching guided distillation. In *ECCV*, 2020.
- [63] Sergey Zagoruyko and Nikos Komodakis. Paying more attention to attention: Improving the performance of convolutional neural networks via attention transfer. In *ICLR*, 2017.

- [64] Y. Zhang, T. Xiang, Timothy M. Hospedales, and H. Lu. Deep mutual learning. In *CVPR*, 2018.
- [65] Borui Zhao, Quan Cui, Renjie Song, Yiyu Qiu, and Jiajun Liang. Decoupled knowledge distillation. In *CVPR*, 2022.
- [66] B. Zhou, A. Khosla, Lapedriza. A., A. Oliva, and A. Torralba. Learning deep features for discriminative localization. In *CVPR*, 2016.

## A Appendix

### A.1 Implementations

**Training details.** On CIFAR-100, we use the same setup as many methods [34, 52]. In particular, the batch size and initial learning rate are set to 64 and 0.05. We train the models for 240 epochs in total with SGD optimizer, and decay the learning rate by 0.1 at 150, 180, and 210 epochs. The weight decay and the momentum are set to  $5e-4$  and 0.9. On ImageNet, following prior works [52, 34], we adopt the SGD optimizer (with 0.9 momentum) to train the student networks for 200 epochs with 256 batch size. The learning rate is set to 0.1, and we decay it by 0.5 every 25 epochs. We set the weight decay to 0.0001. We also apply the vanilla logits distillation loss [22] in our method. For the loss weights in Eq. (3), we set  $\alpha = 0.8$  and  $\beta = 0.2$  for all experiments. The temperature  $\tau$  used on the ImageNet dataset is set to 1.0, and the same parameter on the CIFAR-100 dataset is set to 4.0. The loss weights of each stage is set to 1.0 in the multi-stage feature distillation setting. Our implementation on MS-COCO for object detection follows the same setting used in [59]. We adopt mean squared error (MSE) as the feature distillation loss  $\mathcal{D}_{feat}$ . All experiments are conducted on 8 Tesla V100 GPUs, and our implementation is based on mmdetection framework [6].

**Transformation modules.** We compare some other transformation modules in Table 8, and we give the implementation details of these baselines here.

- **Conv:** Consisting of several convolutional layers, a pooling layer and a fully connected layer.
- **Encoder-Decoder:** We apply ViT [14]-based encoder/decoder in our default transformation module. The encoder [54] consists of 6 blocks, and the decoder consists of 6 blocks for the single stage feature distillation and 4 blocks for the multi-stage feature distillation.  $\mathbf{F}^s$  and  $\mathbf{F}^t$  are encoded by their encoders to form hybrid tokens, and then used as the input of the shared decoder.
- **Decoder:** Different from encoder-decoder,  $\mathbf{F}^s$  and  $\mathbf{F}^t$  do not need to go through their respective encoder networks, but align their feature dimensions through a layer of simple MLP, then add position encoding to form hybrid tokens as the input of the decoder network.

**Details of ConvNeXt-E.** To evaluate the proposed DPK, we conduct experiments (Fig. 4) on the recently published ConvNeXt [37]. We take four ConvNeXt variants, ConvNeXt-T/S/B/L, as teachers to confirm the effectiveness of our method. For this purpose, we build a smaller **ConvNeXt-E** to serve as the student by reducing the blocks/channels in each stage. The other details, such as training strategies, are same as the official models. The configurations are summarized in Table 11. We also report the numbers of parameters, FLOPS, and accuracy for reference.

Table 11: **Detailed settings of ConvNeXt variants.** We also report the parameters, FLOPS and the performance.

	Architecture	Channels	Blocks	#Param.	#FLOPS	Top-1 Acc.	Top-5 Acc.
Student	ConvNeXt-E	(96,192,384,768)	(2,2,4,2)	17.43M	2.6G	77.43%	93.30%
Teacher	ConvNeXt-T	(96,192,384,768)	(3,3,9,3)	28.59M	4.5G	82.06%	95.85%
	ConvNeXt-S	(96,192,384,768)	(3,3,27,3)	50.22M	8.7G	83.15%	96.43%
	ConvNeXt-B	(128,256,512,1024)	(3,3,27,3)	88.59M	15.4G	86.59%	98.19%
	ConvNeXt-L	(192,384,768,1536)	(3,3,27,3)	197.77M	34.4G	87.40%	98.37%

**Details for object detection.** We implement Faster RCNN [47] and RetinaNet [33] with different backbones. To integrate the multi-scale features, FPN [32] is adopted for all experiments. We take FGD [59] (recently published on CVPR’22) as the baseline model, and build our method on it. In particular, the feature distillation loss in FGD can be formulated as follows:

$$\mathcal{L}_{feat} = w_f \text{MSA}^S \text{A}^C (\mathbf{F}^t - f(\mathbf{F}^s))^2 + w_b (1 - M) \text{SA}^S \text{A}^C (\mathbf{F}^t - f(\mathbf{F}^s))^2, \quad (8)$$

where  $\mathbf{F}^s$ ,  $\mathbf{F}^t$  denotes the feature map from student detector and teacher detector, respectively.  $f$  is the adaption layer to reshape the  $\mathbf{F}^s$  to the same dimension as  $\mathbf{F}^t$ .  $M$  is the binary mask, indicating

the foreground and background regions, derived from the ground truth.  $A^S, A^C$  denote the learnable spatial attention map and channel attention map for the teacher detector, respectively.  $S$  is a scale mask used to treat each foreground object identically. Besides,  $w_f$  and  $w_b$  are the hyper-parameters to balance the losses for foreground and background regions. **To combine our model with FGD, we replace  $f$  with Eq. 4, that is, we have,**

$$\mathcal{L}_{feat} = w_f \text{MSA}^S A^C \mathcal{D}_{feat}(\mathbf{F}^t, \mathbf{F}^h) + w_b (1 - M) \text{SA}^S A^C \mathcal{D}_{feat}(\mathbf{F}^t, \mathbf{F}^h), \quad (9)$$

where  $\mathbf{F}^h$  denotes the *hybrid features (tokens)*, whose construction process is stated in the above section. As for the hyper-parameters, such as  $w_f$  and  $w_b$  in Eqn. 9, we follow the settings in FGD [59] and fine-tune them on each training fold. Specifically, we adopt the hyper-parameters  $\{w_f = 5e-5, w_b = 2.5e-5\}$  for all the two-stage detectors, and  $\{w_f = 2e-3, w_b = 5e-4\}$  for all the one-stage detectors. We train all the detectors for 24 epochs with SGD optimizer, with the momentum as 0.9 and the weight decay as 0.0001.

## A.2 More Experiments for Homogeneous Models

**Comparison with TAKD.** TAKD [39] introduces intermediate models as teacher assistants (TAs) to bridge the capacity gap between the teacher models and the student models. This work shares similar motivation with DPK, and we provide experiments to compare these two works. The experiments are based on the ResNet, and we use ResNet-101 as the teacher and ResNet-18 as the student. For TAKD, we adopt ResNet-50 and ResNet-34 as TAs, and then train the TAs and students one by one. For DPK, we directly train the student under the teacher’s guidance. The results are summarized in Table 12. We can find that our DPK surpasses TAKD in performance (e.g. 73.00 v.s. 71.41). Also, note DPK does not need multiple training.

Table 12: **Comparison of DPK and TAKD on ImageNet.** We use ResNet-18 as the student model. For our DPK, we train the student model under the guidance of ResNet-101. For TAKD, we use ResNet-101 as the teacher model, and use ResNet-50 and ResNet-35 as TAs.

Acc.	Baseline (R18)	R101→R50→R34→R18 (TAKD)	R101→R18 (DPK)
Top-1	69.55	71.41	<b>73.00</b>
Top-5	89.09	90.22	<b>90.95</b>

## A.3 More Experiments for Heterogeneous Models

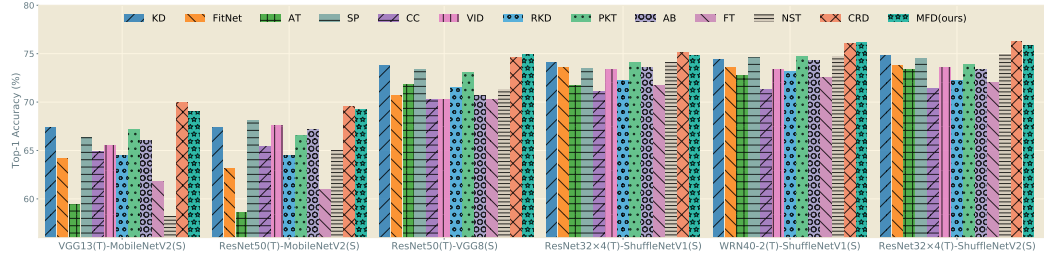


Figure 6: **Heterogeneous experiments on CIFAR-100.** Top-1 accuracy is reported. Best viewed in color with zoom in. “T” denotes the teacher, and “S” denotes the student. Statistically, DPK ranks 1<sup>st</sup> for two pairs and 2<sup>nd</sup> for four pairs.

We report the heterogeneous experiments for some common settings in the main paper. In this section, we give the experiments on CIFAR-100, and more cases on ImageNet.

**Experiments on CIFAR-100.** Fig. 6 presents the experimental results on CIFAR-100. According to these results, we can find our model outperforms all baseline methods across the two model pairs, i.e. ResNet50(T)-VGG8(S) and WRN40-2(T)-ShuffleNetV1(S), and ranks second for the remaining four model pairs, which demonstrates the effectiveness and robustness of DPK. Besides, we also observe that CRD [52] achieves promising performance on this dataset for heterogeneous

Table 13: **Results for heterogeneous models.** We set ResNet18 as the student and networks from EfficientNet [51] series as teachers.

Acc.	Student	EfficientNet-B0	EfficientNet-B1	EfficientNet-B2	EfficientNet-B3	EfficientNet-B4
Top-1	69.55	72.46	73.39	73.81	73.89	74.05
Top-5	89.09	90.56	91.10	91.56	91.63	91.58

Table 14: **ResNet-18 trained with varying teacher models.** We report the top-1 and top-5 accuracy on ImageNet. All teacher models are re-trained by us to adjust their final performances.

Models		#Param.	Teacher Acc. (%)		Student Acc. (%)	
			Top-1	Top-5	Top-1	Top-5
Student	ResNet18	11.69M	–	–	69.55	89.09
Teacher	ResNet34_v1	21.80M	73.31	91.42	70.68	90.16
	ResNet34_v2	21.80M	74.37	91.90	71.36	90.08
	ResNet34_v3	21.80M	75.81	92.70	71.60	90.19
	ResNet34_v4	21.80M	76.27	92.96	71.41	90.22
	ResNet34_v3	21.80M	75.81	92.70	71.60	90.19
	ResNet50_v1	25.56M	75.86	92.88	71.63	90.16
	ResNet101_v1	44.55M	75.97	92.73	71.32	89.95
	ResNet152_v1	60.19M	76.24	92.80	71.21	89.89

settings. Note that our method significantly performs better than CRD for homogeneous settings on CIFAR-100 (see Table 1) and ImageNet (see Table 2) and heterogeneous settings on ImageNet (see Table 3).

**Experiments on ImageNet.** On ImageNet, we adopt EfficientNet [51] as the teacher and ResNet18 as the student to conduct heterogeneous experiments. We only distill the features in the last stage for this experiment. The results shown in Table 13 suggest that DPK also works for other teacher-student pairs, and can be further improved by applying larger models.

#### A.4 Factors Affecting the Effectiveness of KD

In the main paper, we suppose there are two main factors affecting students’ performance: (i) the capacity of the teacher model, and (ii) the performance of the teacher model. We conduct a *toy experiment* to support these two assumptions in this part.

**Performance of the teacher model.** We fix ResNet-18 as students and distill some ResNet-34 from different teachers (*e.g.*, ResNet50) using the vanilla KD [22]. Then we use these ResNet-34 (with different accuracy) as teachers, and report the results in Table 14. We can find better teachers generally lead to better students when the teachers share the same CNN model.

**Capacity of the teacher model.** Similarly, we also select some different distilled ResNet models and keep their performance at a similar level. The results in Table 14 suggest that larger teachers generally degrade the students when the teachers have similar performance.

The above two factors make the choice of the teacher models become a special ‘trade-off’ between accuracy and capacity, and our DPK alleviates this issue by reducing the capacity gap in feature-level.

#### A.5 Visualizations

**CKA curve in training.** To qualitatively analyze the proposed DPK, we take ResNet-18 as the student model, and visualize the CKA similarities trained with four teacher models in the training phase. As shown in Fig. 7, we can find the following two observations: (i) the CKA values increase with training, which demonstrates that our DPK does narrow the gap of teacher-student models at feature level, and (ii) the CKA for the larger teacher is significantly lower than that for small teacher, which suggests the necessity of our dynamic design (observation (i) also support this conclusion). We also visualize the dynamic mask ratios in Fig. 8 for reference.

**Feature similarity before/after distillation.** Here we give more visualizations to show the feature similarity between students and teachers before/after distillation. The feature similarities measured

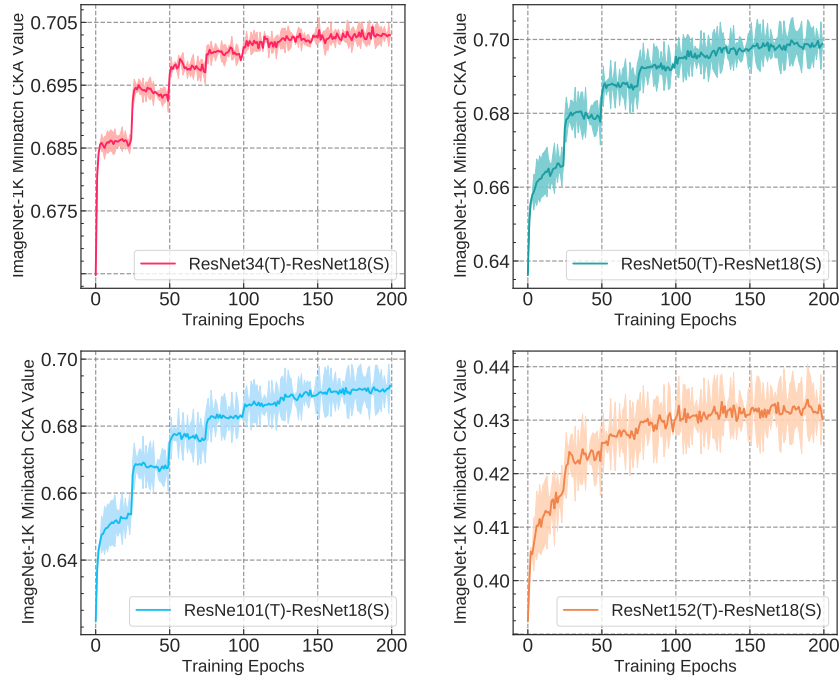


Figure 7: **CKA curves in the training phase.** We visualize the CKA similarities in the training for four teacher-student pairs. The CKA values are computed at the batch-level, and we average them at the epoch-level for better presentation. The corresponding mask ratios to these CKA values are visualized in Fig. 8.

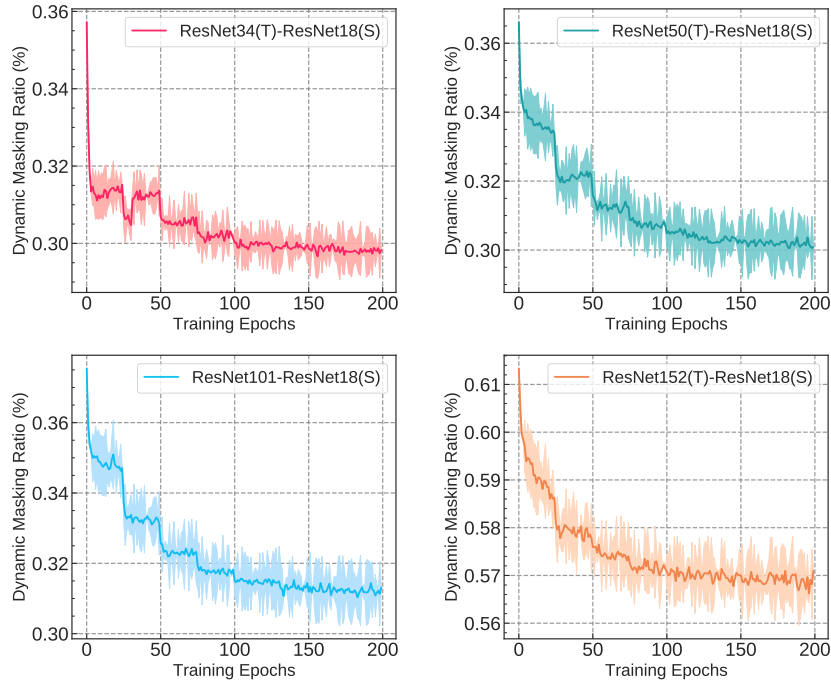


Figure 8: **Dynamic mask ratios.** We visualize the mask ratios dynamically adjusted according to CKA. The mask ratios are adjusted at the batch-level, and we average them at the epoch-level for better presentation. The corresponding CKA curves are visualized in Fig. 7.

by CKA are shown in Fig. 9 and the features similarities measured by Cosine are shown in Fig. 10. These results qualitatively show the effectiveness of our DPK.

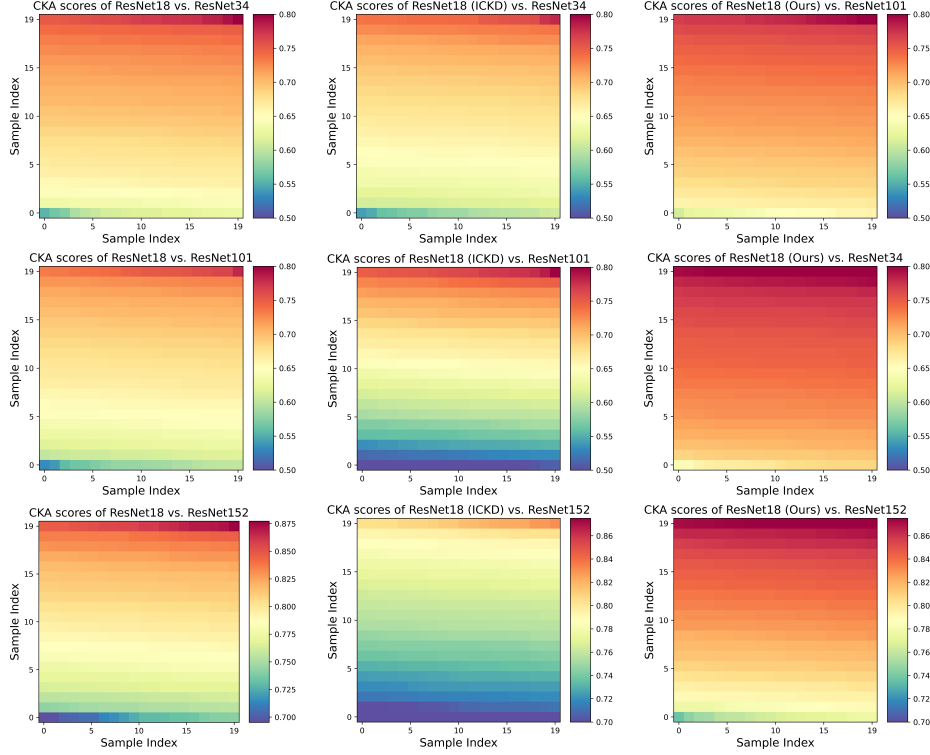


Figure 9: **Feature similarity measured by CKA.** We visualize the CKA similarities for teacher-student pairs before/after distillation. We adopt the same setting used in Fig. 5 for better presentation.

## A.6 Limitations and Discussions

**Limitations.** The Fig. 1, 3, 4 and Table 4, 10, 13 report that the proposed DPK can continue to benefit from larger teacher models. However, we also observe some outliers. In particular, when the teachers of different size belong to different model architectures, the student trained with best teacher may not perform best. For example, the ResNet-18 trained with ConvNeXt-T achieves 71.80 top-1 accuracy on ImageNet (see Figure 4), and then it can achieve 72.51 top-1 accuracy under the guidance of ResNet-34 (see Table 2). Although ConvNeXt-T performs better than ResNet-34, but it provides less guidance to the students. Note that this does not always happen, and we argue that the better teachers still give better results when they belong to the same network family.

**Future work.** This paper investigates a new paradigm for feature distillation, *i.e.* introducing the teacher’s feature to the student as prior knowledge before conducting feature distillation. We show the effectiveness of this idea, meanwhile, this idea can be further explored in future work. For example, we randomly mask the student’s features and fill them with the teacher’s feature. A possible solution is to actively choose the prior knowledge according to some rules, such as the discriminability [66] or uncertainty [25]. Furthermore, different tasks may require different kinds of prior knowledge, *e.g.* object detection may focus more on the foreground features than background features. We hope the idea of this work and the relevant discussions can provide insights to the community.

## A.7 Potential Impacts.

DPK aims to learn more powerful representations for the student model, and theoretically, it can be applied to most CNN-based models and tasks, including these may have negative impacts on the society (*e.g.* face recognition). Besides, same as other data-driven methods, DPK may also give biased results if the models are trained from biased data.

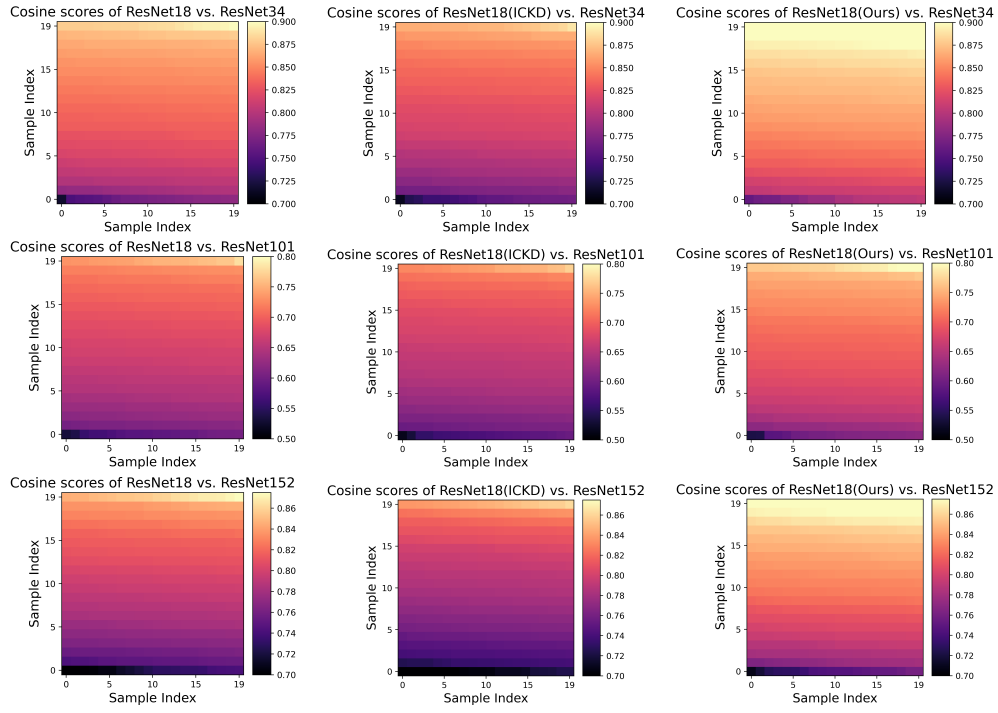


Figure 10: **Feature similarity measured by Cosine distance.** We visualize the cosine similarities for teacher-student pairs before/after distillation. We adopt the same setting used in Fig. 5 for better presentation.